Metal-organic framework mixed-matrix disks: Versatile supports for automated solid-phase extraction prior to chromatographic separation

Metal-organic framework mixed-matrix disks: versatile supports for automated solid-phase extraction prior to chromatographic separation

Milad Ghani,[a,b] Maria Francesca Font Picó,[a] Shima Salehinia,[a,c] Carlos Palomino Cabello,[a] Fernando Maya,[,a] Gloria Berlier,[d] Mohammad Saraji,[b] Víctor Cerdà,[a] Gemma Turnes Palomino*[,a]*

[a.] Department of Chemistry, University of the Balearic Islands, Palma de Mallorca, E-07122, Spain.
[b] Department of Chemistry, Isfahan University of Technology, Isfahan 84156-83111, Iran.
[c] Department of Analytical Chemistry, Faculty of Chemistry, Kashan University, 87317-51167, Kashan, Iran.
[d] University of Torino, Department of Chemistry and NIS Centre, Via P.Giuria 7, 10125 Torino, Italy
**E-mail: fernando.maya@uib.es. *E-mail: g.turnes@uib.es. Fax: (+34) 971 173426. Phone: (+34) 971 173250.*

ABSTRACT

We present for the first time the application of metal-organic framework (MOF) mixed-matrix disks (MMD) for the automated flow-through solid-phase extraction (SPE) of environmental pollutants. Zirconium terephthalate UiO-66 and UiO-66-NH_2 MOFs with different size (90, 200 and 300 nm) have been incorporated into mechanically stable polyvinylidene difluoride (PVDF) disks. The performance of the MOF-MMDs for automated SPE of seven substituted phenols prior to HPLC analysis has been evaluated using the sequential injection analysis technique. MOF-MMDs enabled the simultaneous extraction of phenols with the concomitant size exclusion of molecules of larger size. The best extraction performance was obtained using a MOF-MMD containing 90 nm UiO-66-NH_2 crystals. Using the selected MOF-MMD, detection limits ranging from 0.1 to 0.2 μg L^{-1} were obtained. Relative standard deviations ranged from 3.9 to 5.3% intra-day, and 4.7 to 5.7% inter-day. Membrane batch-to-batch reproducibility was from 5.2 to 6.4%. Three different groundwater samples were analyzed with the proposed method using MOF-MMDs, obtaining recoveries ranging from 90 to 98% for all tested analytes.

Keywords: Metal-organic frameworks; Mixed-matrix disks; Solid-phase extraction; Sequential injection analysis; High performance liquid chromatography; Phenols.

1. Introduction

Metal-organic frameworks (MOFs) are an exciting class of crystalline materials based on the coordination of metal ions or clusters with rigid organic linkers, creating extended ordered networks [1-4]. Due to their large surface area, low density, and tunable composition, MOFs have been widely studied for their use in gas storage [5], separation [6], or catalysis [7]. In the past years the use of MOFs in the analytical chemistry field has been constantly growing [8-11]. MOFs have shown to be promising materials for sampling [12,13], sample preparation [14,15], analyte separation [16-18] and detection [19,20]. For all these applications, MOFs can be used directly, or as templates for other materials, such as carbons, metal oxides or layered double hydroxides [21,22].

However, due to their small size and non-spherical morphology, it is difficult to fully exploit MOFs properties for extraction or separation applications, requiring additional MOF processing strategies such as growth of MOFs on particles [23-26] and monoliths [27-31], or MOF magnetization [32-34]. In addition, MOFs have been incorporated in membranes using different approaches [35-38]. Among them, the entrapment of a high load of well dispersed MOF crystals in a polyvinylidene difluoride (PVDF) matrix, has been recently reported for the preparation of useful membranes for molecular size selective filtration [39].

Among the different types of MOFs, UiO (*Universitetet i Oslo*) MOFs, based on the coordination of zirconium clusters with aromatic carboxylic acids, are excellent candidates for the development of analytical applications due to their high stability [40,41]. The most well-known MOF of the UiO family is the UiO-66, obtained by linking zirconium clusters using terephthalic acid, which contain benzene rings which can interact with other aromatic compounds via π-π interactions. Already reported

applications are the use of the UiO-66 MOF as sorbent for the dispersive solid-phase extraction of polychlorinated biphenyls [42], as fiber coating for solid-phase microextraction [43,44], as coating of magnetic microspheres for magnetic solid-phase extraction [45] or embedded in a polymer monolith for solid-phase microextraction [46].

MOF-polymer composites shaping mixed-matrix membranes have already been explored for the separation of gases [6]. However, these composite materials have not been exploited as supports for solid-phase extraction (SPE) yet. The potential advantages of MOF mixed-matrix supports for SPE are: i) Excellent flow-through properties, enabling SPE applications using MOFs (independently of their crystal size and shape); ii) Simple automation of the SPE process using flow-based techniques, avoiding high backpressures, or the clogging of the flow manifold tubing with small particles; iii) Simple functionalization of the sorbent, just by selecting the appropriate organic linker used in the MOF synthesis; iv) Simple preparation of sorbents enabling the enrichment of target compounds and simultaneously the size exclusion in the desorption step of compounds with a larger molecular size than the pore size of the selected MOF.

The aim of this work is to explore the use of MOF mixed-matrix disks (MMD) as supports for SPE prior to chromatographic separation. Using a polyvinylidene fluoride (PVDF) matrix, disks containing entrapped UiO-66 MOFs (MOF-MMD) have been prepared and characterized. To obtain the best performance for SPE, the effect of the crystal size and chemical composition of the MOFs on the extraction of seven substituted phenols has been studied. The SPE process has been automated using the sequential injection analysis (SIA) technique [47,48], and the extracted phenols have been separated and quantified by means of HPLC analysis, obtaining an efficient method for the preconcentration and separation of the selected analytes from groundwater samples.

2. Experimental

2.1. Chemicals

Acetonitrile (HPLC, ≥99.8%), ethanol (≥99.8%), methanol (≥99.8%), acetone (≥99.8%), isopropanol (≥99.8%), terephthalic acid (99%), N,N-dimethylformamide (DMF, 99.5%), and HCl (37%) were obtained from Scharlau (Barcelona, Spain). Benzoic acid (98%), 4-nitrophenol (4-NP, 98%), 2-chlorophenol (2-CP, 98%), 2,4-dinitrophenol (2,4-DNP, 98%), 2-nitrophenol (2-NP, 98%), 2,4-dimethyl phenol (2,4-DMP, 98%), 4-chloro-3-methyl phenol (4-C-3MP, 98%) and 2,4-dichlorophenol (2,4-DCP, 98%) were obtained from Sigma & Aldrich (St. Louis, USA). Zirconium (IV) chloride ($ZrCl_4$, 98%), was obtained from ACROS (New Jersey, USA). Polyvinylidene difluoride was purchased from a local hardware store.

A stock standard solution of each phenol (2000 mg L^{-1}) was prepared in methanol. An intermediate solution with a concentration of 20 mg L^{-1} of each phenol was prepared by diluting the stock standard solution in water. A standard mixture of phenols (1 mg L^{-1}) was prepared in water. Working solutions were prepared daily by diluting the intermediate solution in water. All solutions were prepared using Milli-Q water (Direct-8 purification system, resistivity >18 MΩ cm, Millipore Iberica, Spain).

2.2. Instrumentation

The SIA system is based on a bi-directional syringe pump (5000-step automatic burette (model Bu4) from Crison, Alella, Barcelona, Spain) equipped with a 5-mL glass syringe from Hamilton (Bonaduz, Switzerland) and a three-way solenoid head valve (SV, N-Research, West Caldwell, NJ). The normally open port (OFF) of the solenoid valve of the syringe is connected to a carrier reservoir, while the normally

closed position (ON) is connected, through a holding coil, to the central port of an eight port multiposition valve (MPV, Sciware Systems SL, Spain), which is used for the selection of the sample, the eluent, and to connect to the extraction device. All tubing is polytetrafluoroethylene (PTFE) 0.8 mm i.d., except the holding coil made of PTFE 1.6 mm i.d. (V= 5 mL).

The extraction device (Sciware Systems SL, **Fig. S1**) is a two-piece polymethyl methacrylate cylinder with an internal cavity to hold the MOF-MMD [49-51]. The prepared disks have a 50 mm diameter. A smaller piece of 10 mm diameter is cut and placed inside the extraction device. The effective extraction area, measured using the dye rhodamine B as tracer is 7 mm. The extraction device is connected to an additional solenoid valve (V5, MTV-3-N1/4UKG, 2 bar maximum nominal pressure, Takasago, Japan) enabling the collection of the eluate into a vial for further HPLC analysis. The additional solenoid valve is controlled by the syringe pump module through an additional port. The syringe pump and the selection valve modules are controlled using the software package AutoAnalysis 5.0 (Sciware Systems SL).

A Jasco HPLC instrument equipped with a high-pressure pump (PU-4180), a manual injector (20 μL), and a UV–Vis diode array detector (MD-4017) was used for the determination of the selected analytes. Separation was performed at room temperature on a Phenomenex® Kinetex EVO C_{18} 100A core-shell column (150 mm × 4.6 mm, i.d. 5 μm) with a guard column (5 mm × 4.6 mm i.d.) from the same material. The mobile phase consisted of acetonitrile (solvent A) and water (solvent B) adjusted to pH 2.8 with sulfuric acid. The gradient program was as follows: 0–3 min, 20% solvent A; 15 min, 55% solvent A; 20 min, 80% solvent A. The mobile phase was used at a flow rate of 1.0 mL min^{-1}. The detection was performed at 200 nm for 2-CP and 2,4-DMP, at 285 nm for 2-NP, 4-C-3MP and 2,4-DNP, at 230 nm for 2,4-DCP, and at 302 nm for 4-NP.

The morphology and elemental distribution of the prepared materials were analyzed by a scanning electron microscope (SEM) Hitachi S-3400N, equipped with a Bruker AXS Xflash 4010 energy-dispersive X-ray spectroscopy (EDS) system. Nitrogen adsorption isotherms were measured at 77 K using a Micromeritics ASAP 2020 physisorption analyzer. All samples were outgassed at 423 K for 6 hours prior to measurement. Data were analyzed using the Brunauer-Emmett-Teller (BET) model to determine the specific surface area. Powder X-ray diffraction (XRD) data were collected using CuKα (λ= 1.54056 Å) radiation o a Siemens D5000 diffractometer.

2.3. Synthesis of UiO-66 and UiO-66-NH_2 MOFs

The different UiO-66 MOFs were prepared by adapting procedures reported in the literature [52-54]. Six UiO-66 samples were prepared with different size and/or functional group of the organic linker using three different preparation methods (solvothermal, microwave and modulated synthesis):

Synthesis of UiO-66. For the solvothermal synthesis of UiO-66, 0.17 g of terephthalic acid were added under constant stirring to 0.25 g of $ZrCl_4$ dissolved in 12 mL of dimethylformamide (DMF) in the Teflon liner of an autoclave. After 5 minutes of additional stirring, the autoclave was placed in an oven for 24 h at 120 ^oC. The obtained solid was filtered and washed thoroughly with ethanol and vacuum dried.

Synthesis of UiO-66-NH_2. The preparation procedure was analogous to that used for the preparation of UiO-66, replacing the terephthalic acid linker by 0.19 g of 2-aminoterephthalic acid.

Microwave synthesis of MW-UiO-66. For the microwave synthesis of UiO-66, 0.15 g of $ZrCl_4$ were dissolved in 40 mL of DMF in the Teflon liner of an autoclave. After 30 min of stirring, 0.12 g of terephthalic acid were added under constant agitation. Reaction was carried out in a microwave oven

(Stard D, Milestone) for 2 h at 120 ^{o}C. The obtained solid was filtered and washed thoroughly with ethanol and vacuum dried.

Microwave synthesis of MW-UiO-66-NH_2. An analogous procedure to that used for the synthesis of MW-UiO-66 was followed, replacing the terephthalic acid by 0.13 g of 2-aminoterephthalic acid.

Modulated synthesis of NP-UiO-66. For the modulated synthesis of UiO-66, 0.24 g of $ZrCl_4$ were dissolved in 18 mL of DMF in an autoclave. 0.16 g of terephthalic acid, 1.22 g of benzoic acid and 0.165 mL of HCl were added under constant stirring. After 5 min of additional stirring, the autoclave was placed in an oven for 48 h at 120 ^{o}C. The obtained solid was filtered and washed thoroughly with ethanol and vacuum dried.

Modulated synthesis of NP-UiO-66-NH_2. The preparation procedure was analogous to that used for the preparation of NP-UiO-66, replacing the terephthalic acid linker by 0.17 g of 2-aminoterephthalic acid.

2.4. Preparation of MOF-MMDs

The MOF-MMDs were prepared adapting a previously reported method [39]. Dry UiO-66 or UiO-66-NH_2 powder was dispersed in 5 mL of acetone (30 mg MOF/mL acetone) by sonicating for 15 min. Then, 1.0 g of a PVDF/DMF solution (7.5 wt. % PVDF) was added to the vial containing the MOF and acetone suspension and sonicated for another 15 min. Thereafter, the acetone was evaporated under a stream of pure nitrogen gas, which resulted in a well dispersed and concentrated MOF-PVDF dispersion in DMF. This final dispersion was casted onto a circular glass Petri Dish (50 mm diameter). After that, solvent was removed by heating at 70 °C for 1 h and the resulting MOF-MMD was delaminated from the glass substrate by immersion in methanol. Finally, the films were thoroughly washed with methanol and dried in air. MOF-MMDs were conditioned with methanol, followed by water, prior to their use as SPE

sorbents. Blank PVDF membranes were prepared in the absence of MOF following the same procedure. The thickness of the prepared disks was approximately 0.1 mm, which is an intermediate thickness between the thickness of other reported MOF mixed-matrix membranes (0.035 mm) [39], and commercial SPE disks based on polystyrene beads entrapped on a PTFE matrix (0.5 mm) [55].

2.5. Samples

In order to study the performance of the developed methodology for real sample analysis, three different water samples were collected from groundwater reservoirs located in the vicinity of different solid waste treatment plants from the Island of Majorca, Spain. All samples were used without any dilution before extraction. The samples were filtered using a nylon membrane filter (0.45 μm, Millipore, Bedford, MA, USA) before use.

2.6. Solid-phase extraction procedure

The SIA system used for the application of MOF-MMDs as sorbents for automated SPE is schematically shown in **Fig. 1a**. The SIA procedure followed for the SPE of phenols is detailed below.

Briefly, an appropriate sample volume (typically 1.5 mL) was loaded into the holding coil through position 2 of the selection valve (SV). The SV was then connected to position 1 and the sample was pumped through the holder containing the MOF-MMD, followed by a volume of carrier to wash the non-retained analytes in the disk. By using an external solenoid valve placed at the outlet of the homemade extraction device, the sample matrix was directed to a waste reservoir. Thereafter, the selection valve was connected to position 3 in order to load an appropriate amount of desorption solvent, and then connected again to position 1 to pump it through the disk desorbing the analytes and, simultaneously, excluding larger molecules if present in the sample (**Fig. 1b**). In this step, the additional solenoid valve

was turned on enabling the collection of the eluate in a vial, for the subsequent HPLC analysis of the extracted analytes. The collected solvent was evaporated under a gentle stream of nitrogen by an off-line procedure and reconstituted in 50 μL of acetone. Finally, a 20 μL portion of the extract was analyzed by HPLC.

3. Results and discussion

3.1. MOF characterization

The six different UiO samples prepared were characterized by powder X-ray diffraction (XRD), scanning electron microscopy (SEM) and nitrogen physisorption in order to study their structural, morphological and textural properties.

The XRD patterns and SEM images of the synthesized samples are shown in **Fig. 2**. The X-ray diffractograms of all the UiO-66 (**Fig. 2a**) and UiO-66-NH_2 (**Fig. 2e**) samples showed good crystallinity and were in good agreement with the theoretical diffraction pattern of the UiO-66 structure obtained from crystallographic data reported by Zhao et al. [56], demonstrating that in all cases pure phase UiO MOFs were obtained.

The morphology and the average crystallite size were determined using SEM (**Figs. 2b** to **2d** and **2f** to **2h**). Electronic micrographs show that all the samples, regardless of the preparation method used, were formed by aggregates of particles with globular shape and different size. Solvothermal synthesis produced materials with an average size of approximately 300 nm **(Figs. 2b** and **2f)**, while in the case of microwave-assisted synthesis (**Fig. 2c** and **Fig. 2g)**, smaller particles of approximately 200 nm were obtained. Nanoparticles, with an approximate size of 90 nm, were obtained using a modulated synthesis

approach for the termination of the MOF crystal growth at an earlier stage by the addition of benzoic acid (**Fig. 2d** and **Fig. 2h**).

Nitrogen adsorption isotherms at 77 K are shown in **Fig. S2**. The obtained BET specific surface areas decreased in the following order: NP-UiO-66 (1251 m^2/g) > NP-UiO-66-NH_2 (1238 m^2/g) > MW-UiO-66 (1031 m^2/g) > MW-UiO-66-NH_2 (1028 m^2/g) > UiO-66 (938 m^2/g) > UiO-66-NH_2 (928 m^2/g), being this decrease probably related to the corresponding increase in the particle size.

3.2. Selection of optimum MOF-MMD for the extraction of phenols

The aim of this study is to select the MOF-MMD with the best extraction performance for the automated SPE of substituted phenols from waters. As a preliminary experiment, the prepared bulk MOFs were used as sorbents for the extraction of the dye rhodamine B under batch conditions. 100 mg of each of the prepared bulk UiOs were added into 100 mL of a 10 mg L^{-1} rhodamine B aqueous solution. After stirring for 15 min, the remaining rhodamine B in solution was measured using UV-Vis spectrophotometry. The trend for the extraction of rhodamine B in batch using the bulk UiOs is shown in **Fig. 3a**. A remarkable increase on the extraction of rhodamine B was observed by decreasing the particle size of the UiO. When UiOs with similar size and different linker are compared, UiOs obtained using the 2-aminoterephthalic acid as ligand showed a superior extraction performance.

The prepared UiO MOFs were then entrapped in PVDF matrices, and studied as sorbents for the automated SPE of seven substituted phenols (4-NP, 2-CP, 2,4-DNP, 2-NP, 2,4-DMP, 4-C-3-MP and 2,4-DCP). The performance for the extraction of phenols (**Fig. 3b**) improved slightly after SPE using a bare PVDF disk as sorbent, in comparison with the direct injection of phenols. When SPE was performed using MOF-MMDs the extraction performance improved considerably. This improvement on the extraction of phenols is attributed to the existence of π-π interactions between the aromatic rings of the

phenols and the aromatic rings of the terephthalic acid linkers in the UiO framework, although the Zr-O sites present in the UiO MOFs and the amino groups of the organic linker used in the preparation of the UiO-66-NH_2 series could also contribute to the extraction process. The best extraction performance for all the tested MOFs was obtained by using the MOF with the smallest particle size, and the highest surface area, and containing amino functional groups. According to this, the NP-UiO-66-NH_2 MMD was selected for the study of the extraction variables and the development of further applications for real sample analysis.

Characterization results of the UiO-MMD containing NP-UiO-66-NH_2 crystals are shown in **Fig. 4**. **Fig. 4a** shows a SEM micrograph of the bare PVDF disk prepared in the absence of MOFs. SEM micrographs at different magnifications of the MOF-MMD (**Fig. 4b** and **Fig. 4c**) show that the NP-UiO-66-NH_2 crystals are well integrated with the polymer binder forming a dense packing. The X-ray diffraction pattern of the UiO-MMD (**Fig. 4d**) shows intense peaks matching well with those of the bulk compound (**Fig. 2e**) and those of the simulated pattern of the bulk material obtained from the crystallographic data reported by Zhao et al. [56], corroborating that, as also shown by SEM (**Fig. 4c**), MOFs crystals remain intact after mixing with the PVDF. EDS spectrum shows an intense Zr band while no zirconium is detected in the bare disk, demonstrating the presence of this element in the UiO-MMD (**Fig. 4f**). In addition, elemental EDS mapping (**Fig. 4e**) shows the homogeneous distribution of Zr in the MOF-MMDs. As it can be observed in **Fig. 4g**, where a detailed cross-section SEM image of the UiO-MMD is shown, the total thickness of the disk is around 100 μm. A higher magnification of the cross-section of the MOF-MMD (**Fig. 4h**) shows the coexistence of both UiO crystals and the PDVF matrix, corroborating the good integration of MOF particles into the polymer.

3.3. Selection of the solvent for analyte desorption from the MOF-MMD

Different organic solvents were studied in order to obtain the best desorption conditions of the analytes from the MOF-MMD. **Fig. 5** shows the effect of methanol, ethanol, isopropanol, acetonitrile and acetone on the desorption of the analytes from the NP-UiO-66-NH_2-MMD. All solvents tested were appropriated for the desorption of the different analytes. However, the best desorption performance was obtained using acetone. Therefore, acetone was selected as desorption solvent for further experiments.

In order to ensure analyte desorption from the MOF-MMD all desorption solvent mixtures were prepared containing 0.1 mmol L^{-1} NaOH, which also prevented the loss of analyte during the solvent evaporation process. However, the concentration of added NaOH need to be selected carefully in order to avoid damage of the used stationary phase material in the further chromatographic analysis of the SPE extract.

3.4. Study of the extraction parameters

Sample volume, desorption solvent volume, and flow rates for the extraction and desorption steps are critical parameters for the development of SPE procedures performed by flow-based techniques working under non-equilibrium conditions.

Fig. 6a shows the influence of the sample volume on the preconcentration of phenols. Under the selected experimental conditions, the extracted quantity of all analytes increased while increasing the sample volume from 0.5 mL to 2.0 mL. Using a sample volume of 2 mL, apparent breakthrough was observed for 4-NP and 2-NP. A volume of 1.5 mL of sample was subsequently adopted to perform further experiments, in a compromise between an appropriate sensitivity and a high extraction throughput.

Fig. 6b shows the effect of the desorption solvent volume on the elution of the extracted phenols from the MOF-MMD disk. The desorption solvent volume was studied from 0.1 mL to 0.5 mL in order to minimize solvent consumption in the desorption step, while ensuring the efficient desorption of the

retained analytes from the SPE support. The performance of the method increased by increasing the desorption solvent volume up to a volume of 0.3 mL. The use of larger volumes (0.5 mL) did not led to any further improvement. Therefore a desorption solvent volume of 0.3 mL was selected for further experiments.

The effect of the sample extraction flow rate was studied in the range from 0.3 mL min^{-1} (minimum volume allowed by the syringe pump equipped with a 5 mL syringe) to 1.5 mL min^{-1}. **Fig. 6c** shows a slight decrease of analyte extraction at higher flow rates. The increase of the sample flow rate decreases the contact time between the analytes and the MOF-MMD, decreasing the mass transfer, and therefore, the extracted quantity of analyte. In a compromise between a high extraction efficiency and a high extraction throughput, a flow rate for the extraction step of 1 mL min^{-1} was adopted for further experiments. **Fig. 6d** shows the effect of the desorption solvent flow rate on the desorption of the retained analytes from the MOF-MMD. The effect of the flow rate on the desorption step follows a similar trend to that of the extraction step. When increasing the desorption solvent flow rate, the contact time between the desorption solvent and the sorbent with the retained analytes decreases, decreasing as well the action of the solvent on the desorption process. The effect of the desorption solvent flow rate was studied from 0.3 mL min^{-1} to 1.5 mL min^{-1}. The highest flow rate that enabled the maximum efficiency on the desorption step was 0.5 mL min^{-1}, being so adopted for further experiments.

The effect of the sample pH was also considered due to the ionizable nature of the analytes, as well as to possible changes on the surface charge of the MOF embedded in the PVDF disk. As shown in **Fig. S3**, pH did not have a significant effect on the extracted quantity, when varied from pH= 4 to pH= 8. Two of the studied analytes are acidic phenolic compounds (2,4-DNP, pKa 4.11; 2-NP, pKa 4.89) while four of them are basic phenols (2,4-DCP, pKa 8.9; 2-CP, pKa 9.26; 4-C-3-MP, pKa 9.71; 2,4-DMP, pKa 10.6). For these analytes, the influence of the pH of the sample in the considered range is

almost negligible. However, the influence of the pH of the sample is more noticeable for the 4-NP (pKa 7.16), observing a decrease on the extracted quantity of this analyte when the extraction is performed at pH= 8. Therefore, the sample pH was maintained at pH= 6 for further extraction studies.

The slight effect of the pH value on phenols extraction indicates that, in the range of pH evaluated, the adsorption of phenols is not much influenced by the ionic state of the analytes or the net charge of the MOF surface, suggesting that, as stated before, in spite of electrostatic interactions, the improvement on the extraction capacity for phenols of the MOF-MMDs is mostly due to the existence of π-π interactions between the aromatic rings of the phenols and the aromatic rings of the terephthalic acid linkers in the UiO framework [31,43]. However, contributions from other kind of interactions, like hydrogen bonding between the amino groups and the functional groups of some of the phenols and between the hydroxyl groups of the phenols and the the Zr-O sites of the MOFs, cannot be neglected.

3.5. Analytical features

The analytical features for the developed SIA method for the extraction of phenols using NP-UiO-66-NH_2-MMDs, followed by analyte quantification by HPLC, are summarized in **Table 1**. The linear dynamic range comprising all analytes was from 0.5 μg L^{-1} to 500 μg L^{-1}, with an acceptable linearity according to the obtained determination coefficients r^2 ranging from 0.990 to 0.999. The LOD values were calculated at a signal-to-noise (S/N) ratio of 3 and ranged from 0.1 μg L^{-1} to 0.2 μg L^{-1}.

The relative standard deviations (RSD, n= 6) for different injections using identical experimental conditions and the same MOF-MMD were examined at two different concentration levels (10 and 100 μg L^{-1}), obtaining RSD ranging from 3.9% to 5.7% in all instances. The inter-day RSD was calculated from extractions performed at 6 different days using MOF-MMDs from the same batch. In this case, inter-day RSDs ranged from 4.7% to 5.7%. MOF-MMD batch-to-batch reproducibility was stablished as

292 the RSD calculated from extractions performed using three different PVDF-MOF batches. In this case,
293 the obtained batch-to-batch reproducibilities ranged from 5.2% to 6.4%. The preconcentration factor was
294 defined as the ratio of the peak area of the measured analytes after extraction using the MOF-MMD, to
295 the initial concentration of the analytes in the aqueous sample solution. The obtained preconcentration
296 factors ranged from 12 to 20, under the selected extraction conditions and using a sample volume of 2
297 mL. The MOF-MMD could be reused at least 40 times without loss of extraction capacity. The extraction
298 throughput under the selected experimental conditions and using a sample volume of 1.5 mL was 16 h^{-1}.
299
300 *3.6. Sample analysis*

301 In order to study the applicability of the developed MOF-MMDs for the SPE of substituted phenols, three
302 different potentially polluted groundwater samples were analyzed. Groundwater samples came from
303 water reservoirs located near different solid waste treatment plants. Analyte quantification was performed
304 using the standard addition method. Samples were spiked with the analytes at three different
305 concentration levels (1, 2 and 5 μg L^{-1}). Recovery studies were performed by spiking the samples with
306 a concentration of 5 μg L^{-1} of each analyte. Analyte recoveries were calculated as the ratio of the
307 concentration of the analyte measured in the spiked samples and in pure water spiked at the same
308 concentration level. The obtained results are shown in **Table 2**. After spiking, the obtained recoveries
309 ranged from 90% to 98%, for all the samples analyzed. These results confirm the suitability of the MOF-
310 MMDs for real sample analysis.

311 **Fig. 7** shows an example of HPLC chromatogram of the selected phenols. The direct injection of
312 a standard containing 5 μg L^{-1} of each analyte plus 250 μg L^{-1} of a molecule with a larger molecular size
313 (thionin dye was used as example) showed how just thionin and 2-CP can be directly detected at this
314 concentration level. Using the bare PVDF disk, a certain preconcentration degree was attained when

analyzing the groundwater sample 3, increasing both the peak intensities of the larger and smaller molecules. In this case, all compounds spiked into the sample where detected except the 2-NP and the 2,4-DMP. Using the MOF-MMD containing NP-UiO-66-NH_2 crystals for SPE, all seven analytes are clearly detected. However, the larger molecule thionin was retained in the MOF-MMD, not being desorbed during the desorption step under the selected conditions, as shown by the blue color of the extraction area of the disk after the extraction step. This result confirms the size exclusion capacity of MOF-MMDs. Note that part of the thionin was transferred in the desorption step using the bare PVDF disk.

UiO-66 MOFs were explored previously for the extraction of phenols by fabricating a UiO-66 coated fiber [44]. By using GC with flame ionization detection, a mixture of 6 phenols were determined in river water samples at the μg L^{-1} level. The obtained limits of detection ranged from 0.11 to 1.23 μg L^{-1}. The proposed method using MOF-MMDs for the SPE of phenols have a comparable performance with the already reported method, with the advantage of the automation of the SPE process. Furthermore, the size exclusion capacity of the developed SPE support provides additional advantages for chemical analysis, such as: increased selectivity for small molecule analysis, simplification of the sample matrix prior to the injection into chromatographic instrumentation, and improved selectivity for chemical analysis using non-chromatographic techniques. The main drawbacks on the use of MOF-MMDs as sorbents for SPE are the limited availability of commercially available MOFs, and the generally limited stability of MOFs in acidic medium. However, many MOFs can be synthesized easily from cheap commercially available precursors, and are stable to the experimental conditions used in many typical SPE applications.

The former advantages, together with their simple and versatile preparation and facile automation, give MOF-MMDs a plethora of possibilities for analytical sample preparation.

4. Conclusions

In this study, the use of metal-organic framework mixed-matrix disks (MOF-MMD) as sorbents for SPE has been explored for the first time. Different MOFs from the UiO family, with a different size and/or organic linker, were embedded in PVDF matrices, shaping small disks for SPE. MOF-MMDs showed excellent flow-through features, enabling the automation of the SPE process using a low-pressure SIA analyzer. The developed MOF-MMDs showed high performance for the automated SPE of seven different substituted phenols and the possibility of size exclusion of larger molecules present in the samples, which is also a characteristic of potential interest in other fields of chemical analysis. A gradual increase in the extraction performance for phenols was obtained while decreasing the crystal size of the prepared UiO-66 MOFs. In addition, the incorporation of amino groups in the organic linker of the MOF favored the further improvement of the extraction process. Multiple possibilities for extraction are opened by embedding MOFs in polymer matrices, due to the plethora of available MOFs containing different metals and organic linkers, as well as to their size and shape tunability. Future research using MOF-MMDs can be directed to the study of the incorporation of other MOFs, the preparation of MOF-MMDs with different morphologies, or the use of MOF-MMDs as precursors for the in situ conversion of the MOFs to other functional materials, such as metal oxides or layered double hydroxides.

Acknowledgments

The Spanish Ministerio de Economía y Competitividad (MINECO) and the European Funds for Regional Development (FEDER) are gratefully acknowledged for financial support through Project CTQ2013-47461-R. F.M. acknowledges the support of the Government of the Balearic Islands and the European

Social Fund for a postdoctoral fellowship and the Acció Especial number AAEE/35. M.G. acknowledges the support of the Ministry of Science of Iran for his financial support.

Supplementary data

A representation of the extraction device used to hold the MOF-MMD, adsorption isotherms of the prepared UiO-66 and UiO-66-NH_2 MOFs, and the effect of pH sample on the extraction capacity of phenols of the NP-UiO-66-NH_2-MMD.

References

[1] O.M. Yaghi, M. O'Keeffe, N.W. Ockwig, H.K. Chae, M. Eddaoudi, J. Kim, Reticular synthesis and the design of new materials. Nature 423 (2003) 705-714.

[2] S. Kitagawa, R. Kitaura, S.I. Noro, Functional porous coordination polymers. Angew. Chem. Int. Ed. 43 (2004) 2334-2375.

[3] G. Férey, Hybrid porous solids: past, present, future. Chem. Soc. Rev. 37 (2008) 191-214.

[4] H. Furukawa, K.E. Cordova, M. O'Keeffe, O.M. Yaghi, The chemistry and applications of metal-organic frameworks. Science 341 (2013) 123044.

[5] A.R. Millward, O.M. Yaghi, Metal−organic frameworks with exceptionally high capacity for storage of carbon dioxide at room temperature. J. Am. Chem. Soc. 127 (2005) 17998-17999.

[6] J.R. Li, J. Sculley, H.C. Zhou, Metal–organic frameworks for separations. Chem. Rev. 112 (2011) 869-932.

[7] A. Corma, H. García, F.X. Labres i Xamena, Engineering metal organic frameworks for heterogeneous catalysis. Chem. Rev. 110 (2010) 4606-4655.

[8] Z.Y. Gu, C.X. Yang, N.A. Chang, X.P. Yan, Metal–organic frameworks for analytical chemistry: from sample collection to chromatographic separation. Acc. Chem. Res. 45 (2012) 734-745.

[9] Y. Yu, Y. Ren, W. Shen, H. Deng, Z. Gao, Applications of metal-organic frameworks as stationary phases in chromatography. Trends Anal. Chem. 50 (2013) 33-41.

[10] P. Kumar, A. Deep, K.H. Kim, Applications of metal-organic frameworks as stationary phases in chromatography. Trends Anal. Chem. 73 (2015) 39-53.

[11] P. Rocío-Bautista, I. Pacheco-Fernández, J. Pasán, V. Pino, Are metal-organic frameworks able to provide a new generation of solid-phase microextraction coatings?–A review. Anal. Chim. Acta 939 (2016) 26-41.

[12] Z.Y. Gu, G. Wang, X.P. Yan, MOF-5 Metal−organic framework as sorbent for in-field sampling and preconcentration in combination with thermal desorption GC/MS for determination of atmospheric formaldehyde. Anal. Chem. 82 (2010) 1365-1370.

[13] Y. Hu, H. Lian, L. Zhou, G. Li, In situ solvothermal growth of metal–organic framework-5 supported on porous copper foam for noninvasive sampling of plant volatile sulfides. Anal. Chem. 87 (2014) 406-412.

[14] L. Xie, S. Liu, Z. Han, R. Jiang, H. Liu, F. Zhu, F. Zeng, C. Su, G. Ouyang, Preparation and characterization of metal-organic framework MIL-101 (Cr)-coated solid-phase microextraction fiber. Anal. Chim. Acta 853 (2015) 303-310.

[15] F. Maya, C.P. Cabello, S. Clavijo, J.M. Estela, V. Cerdà, G.T. Palomino, Zeolitic imidazolate framework dispersions for the fast and highly efficient extraction of organic micropollutants. RSC Adv. 5 (2015) 28203-28210.

[16] B. Chen, C. Liang, J. Yang, D.S. Contreras, Y.L. Clancy, E.B. Lobkovsky, O.M. Yaghi, S. Dai, A microporous metal-organic framework for gas-chromatographic separation of alkanes. Angew. Chem. Int. Ed. 45 (2006) 1390-1393.

[17] X. Kuang, Y. Ma, H. Su, J. Zhang, Y.B. Dong, B. Tang, High-performance liquid chromatographic enantioseparation of racemic drugs based on homochiral metal–organic framework. Anal. Chem. 86 (2014) 1277-1281.

[18] C.X. Yang, X.P. Yan, Metal–organic framework MIL-101 (Cr) for high-performance liquid chromatographic separation of substituted aromatics. Anal. Chem. 83 (2011) 7144-7150.

[19] C.X. Yang, H.B. Ren, X.P Yan, Fluorescent metal–organic framework MIL-53 (Al) for highly selective and sensitive detection of Fe^{3+} in aqueous solution. Anal. Chem. 85 (2013) 7441-7446.

[20] Y. Dong, J. Cai, Q. Fang, X. You, Y. Chi, Dual-emission of lanthanide metal–organic frameworks encapsulating carbon-based dots for ratiometric detection of water in organic solvents. Anal. Chem. 88 (2016) 1748-1752.

[21] L. Hao, C. Wang, Q. Wu, Z. Li, X. Zang, Z. Wang, Metal–organic framework derived magnetic nanoporous carbon: novel adsorbent for magnetic solid-phase extraction. Anal. Chem. 86 (2014) 12199-12205.

[22] M. Ghani, R.M. Frizzarin, F. Maya, V. Cerdà, In-syringe extraction using dissolvable layered double hydroxide-polymer sponges templated from hierarchically porous coordination polymers. J. Chromatogr. A 1453 (2016) 1-9.

[23] R. Ameloot, A. Liekens, L. Alaerts, M. Maes, A. Galarneau, B. Coq, G. Desmet, B.F. Sels, J.F. Denayer, D.E. De Vos, Silica–MOF composites as a stationary phase in liquid chromatography. Eur. J. Inorg. Chem. 24 (2010) 3735-3738.

[24] S. Sorribas, B. Zornoza, C. Téllez, J. Coronas, Ordered mesoporous silica–(ZIF-8) core–shell spheres. Chem. Commun. 48 (2012) 9388-9390.

[25] F. Maya, C.P. Cabello, S. Clavijo, J.M. Estela, V. Cerdà, G.T. Palomino, Automated growth of metal–organic framework coatings on flow-through functional supports. Chem. Commun. 51 (2015) 8169-8172.

[26] S. Sorribas, B. Zornoza, P. Serra-Crespo, J. Gascon, F. Kapteijn, C. Téllez, J. Coronas, Synthesis and gas adsorption properties of mesoporous silica-NH_2-MIL-53(Al) core–shell spheres. Micropor. Mesopor. Mat. 225 (2016) 116-121.

[27] Y.Y. Fu, C.X. Yang, X.P. Yan, Incorporation of metal–organic framework UiO-66 into porous polymer monoliths to enhance the liquid chromatographic separation of small molecules. Chem. Commun. 2013, 49, 7162-7164.

[28] A. Saeed, F. Maya, D.J. Xiao, M. Najam-ul-Haq, F. Svec, D.K. Britt, Growth of a highly porous coordination polymer on a macroporous polymer monolith support for enhanced immobilized metal ion affinity chromatographic enrichment of phosphopeptides Adv. Funct. Mater. 24 (2014) 5790-5797.

[29] A. Lamprou, H. Wang, A. Saeed, F. Svec, D.K. Britt, F. Maya, Preparation of highly porous coordination polymer coatings on macroporous polymer monoliths for enhanced enrichment of phosphopeptides. J. Vis. Exp. 101 (2015) e52926-e52926.

[30] L. Wen, A. Gao, Y. Cao, F. Svec, T. Tan, Y. Lv, Layer-by-layer assembly of metal–organic frameworks in macroporous polymer monolith and their use for enzyme immobilization. Macromol. Rapid Commun. 37 (2016) 551-557.

[31] Y. Lv, X. Tan, F. Svec, Preparation and applications of monolithic structures containing metal–organic frameworks. J. Sep. Sci. (2016) DOI: 10.1002/jssc.201600423.

[32] F. Maya, C.P. Cabello, J.M. Estela, V. Cerdà, G.T. Palomino, Automatic in-syringe dispersive microsolid phase extraction using magnetic metal–organic frameworks. Anal. Chem. 87 (2015) 7545-7549.

[33] S.H. Huo, X.P. Yan, Facile magnetization of metal–organic framework MIL-101 for magnetic solid-phase extraction of polycyclic aromatic hydrocarbons in environmental water samples. Analyst 137(2012) 3445-3451.

[34] P. Rocío-Bautista, V. Pino, J.H. Ayala, J. Pasán, C. Ruiz-Pérez, A.M. Afonso, A magnetic-based dispersive micro-solid-phase extraction method using the metal-organic framework HKUST-1 and ultra-high-performance liquid chromatography with fluorescence detection for determining polycyclic aromatic hydrocarbons in waters and fruit tea infusions. J. Chromatogr. A 1436 (2016) 42-50.

[35] S.R. Venna, M.A. Carreon, Highly permeable zeolite imidazolate framework-8 membranes for CO_2/CH_4 separation. J. Am. Chem. Soc. 132 (2009) 76-78.

[36] T.H. Bae, J.S. Lee, W. Qiu, W.J. Koros, C.W. Jones, S. Nair, A high-performance gas-separation membrane containing submicrometer-sized metal–organic framework crystals. Angew. Chem. Int. Ed. 49 (2010) 9863-9866.

[37] T. Rodenas, I. Luz, G. Prieto, B. Seoane, H. Miro, A. Corma, F. Kapteijn, F.X.L. Xamena, J. Gascon, Nat. Mater. 14 (2015) 48-55.

[38] N.C. Su, D.T. Sun, C.M. Beavers, D.K. Britt, W.L. Queen, J.J. Urban, Enhanced permeation arising from dual transport pathways in hybrid polymer–MOF membranes. Energy Environ. Sci. 9 (2016) 922-931.

[39] M.S. Denny, S.M. Cohen, In situ modification of metal–organic frameworks in mixed-matrix membranes. Angew. Chem. Int. Ed. 54 (2015) 9029-9032.

[40] J.H. Cavka, S. Jakobsen, U. Olsbye, N. Guillou, C. Lamberti, S. Bordiga, K.P. Lillerud, A new zirconium inorganic building brick forming metal organic frameworks with exceptional stability. J. Am. Chem. Soc. 130 (2008) 13850-13851.

[41] M. Kandiah, M.H. Nilsen, S. Usseglio, S. Jakobsen, U. Olsbye, M. Tilset, C. Larabi, E.A. Quadrelli, F. Bonino, K.P. Lillerud, Synthesis and stability of tagged UiO-66 Zr-MOFs. Chem. Mater. 22 (2010) 6632-6640.

[42] S. Lin, N. Gan, Y. Cao, Y. Chen, Q. Jiang, Selective dispersive solid phase extraction-chromatography tandem mass spectrometry based on aptamer-functionalized UiO-66-NH_2 for determination of polychlorinated biphenyls. J. Chromatogr. A 1446 (2016) 34-40.

[43] J. Gao, C. Huang, Y. Lin, P. Tong, L. Zhang, In situ solvothermal synthesis of metal–organic framework coated fiber for highly sensitive solid-phase microextraction of polycyclic aromatic hydrocarbons. J. Chromatogr. A 1436 (2016) 1-8.

[44] H.B. Shang, C.X. Yang, X.P. Yan, Metal–organic framework UiO-66 coated stainless steel fiber for solid-phase microextraction of phenols in water samples. J. Chromatogr. A 1357 (2014) 165-171.

[45] W. Zhang, Z. Yan, J. Gao, P. Tong, W. Liu, L. Zhang, Metal–organic framework UiO-66 modified magnetite@silica core–shell magnetic microspheres for magnetic solid-phase extraction of domoic acid from shellfish samples. J. Chromatogr. A 1400 (2015) 10-18.

[46] C.L. Lin, S. Lirio, Y.T. Chen, C.H. Lin, H.Y. Huang, A novel hybrid metal–organic framework–polymeric monolith for solid-phase microextraction. Chem. Eur. J. 20 (2014) 3317-3321.

[47] J. Ruzicka, G.D. Marshall, Sequential injection: a new concept for chemical sensors, process analysis and laboratory assays. Anal. Chim. Acta 237 (1990) 329-343.

[48] C.E. Lenehan, N.W. Barnett, S.W. Lewis, Sequential injection analysis. Analyst 127 (2002) 997-1020.

[49] C. Pons, R. Forteza, V. Cerdà, The use of anion-exchange disks in an optrode coupled to a multi-syringe flow-injection system for the determination and speciation analysis of iron in natural water samples. Talanta 66 (2005) 210-217.

[50] F. Maya, J.M. Estela, V. Cerdà, Interfacing on-line solid phase extraction with monolithic column multisyringe chromatography and chemiluminescence detection: An effective tool for fast, sensitive and selective determination of thiazide diuretics. Talanta 80 (2010) 1333-1340.

[51] F. Maya, J.M. Estela, V. Cerdà, Completely automated system for determining halogenated organic compounds by multisyringe flow injection analysis. Anal. Chem. 80 (2008) 5799-5805.

[52] S.J. Garibay, S.M. Cohen, Isoreticular synthesis and modification of frameworks with the UiO-66 topology. Chem. Commun. 46 (2010) 7700-7702.

[53] Y. Li, Y. Liu, W. Gao, L. Zhang, W. Liu, J. Lu, Z. Wang, Y.J. Deng, Microwave-assisted synthesis of UIO-66 and its adsorption performance towards dyes. CrystEngComm 16 (2014) 7037-7042.

[54] X. Zhu, J. Gu, Y. Wang, B. Li, Y. Li, W. Zhao, J. Shi, Inherent anchorages in UiO-66 nanoparticles for efficient capture of alendronate and its mediated release. Chem. Commun. 50 (2014) 8779-8782.

[55] http://solutions.3m.com/wps/portal/3M/en_US/Empore/extraction/products/disks. Last accessed, June 2016.

[56] Q. Zhao, W. Yuan, J. Liang, J. Li, Synthesis and hydrogen storage studies of metal-organic framework UiO-66. Int. J. Hydrogen Energy 38 (2013) 13104-13109.

Table 1. Analytical features for the automated SPE of substituted phenols using the MOF-MMD based on NP-UiO-66-NH_2 crystals.

Analyte	Linear range (µg L^{-1})	Determination Coefficient (r^2)	LOD (µg L^{-1})	Precision (%)[a]				PF[d]
				Intra-day		Inter-day 50 (µg L^{-1})	Batch-to-batch reproducibility[c] 50 (µg L^{-1})	
				100 (µg L^{-1})[b]	10 (µg L^{-1})			
4-NP	0.5-500	0.990	0.2	4.9	5.3	5.7	5.9	20
2-CP	0.5-200	0.999	0.1	4.6	4.9	5.3	5.7	13
2,4-DNP	0.5-200	0.996	0.2	4.3	4.7	5.4	6.3	12
2-NP	0.5-100	0.998	0.1	3.9	4.1	4.7	6.4	18
2,4-DMP	0.5-200	0.996	0.2	4.5	4.9	5.3	5.2	16
4-C-3-MP	0.5-200	0.996	0.2	4.7	5.2	5.6	5.4	14
2,4-DCP	0.5-200	0.998	0.2	5.1	5.3	5.5	5.9	10

[a] Relative standard deviation (n= 6).
[b] Spiking level.
[c] Batch-to-batch reproducibility was calculated by analysing water samples spiked at 50 µg L^{-1} using three different MOF-MMDs prepared under the same conditions.
[d] Preconcentration factor

Table 2. Analysis of phenols from groundwater samples using automated SPE followed by HPLC analysis using the MOF-MMD based on NP-UiO-66-NH_2 crystals.

Compound	Sample 1			Sample 2			Sample 3		
	Measured (µg L^{-1})	Found[a] (µg L^{-1})	Recovery (%)	Measured (µg L^{-1})	Found (µg L^{-1})	Recovery (%)	Measured (µg L^{-1})	Found (µg L^{-1})	Recovery (%)
4-NP	1.5	6.3	96	ND	4.7	94	ND	4.8	96
2-CP	1.2	5.8	92	1.8	6.4	92	ND	4.9	98
2,4-DNP	ND	4.8	96	ND	4.6	92	ND	4.7	94
2-NP	ND	4.9	98	ND	4.7	94	ND	4.6	92
2,4-DMP	1.4	6.1	94	0.6	5.4	96	ND	4.9	98
4-C-3-MP	1.5	6.1	94	ND	4.7	94	ND	4.5	90
2,4-DCP	0.9	5.5	92	2.1	6.8	94	ND	4.6	92

[a] Spiking level, 5 µg L^{-1} of each analyte

Figure captions

Figure 1. Representation of the developed set-up for the implementation of MOF-MMDs for automated SPE (a), and the SPE process using MOF-MMDs (b).

Figure 2. XRD pattern of the synthesized UiO-66 samples (a). SEM images of the prepared UiO-66 (b), MW-UiO-66 (c) and NP-UiO-66 (d). XRD pattern of the synthesized UiO-66-NH_2 samples (e). SEM images of the prepared UiO-66-NH_2 (f), MW-UiO-66-NH_2 (g) and NP-UiO-66-NH_2 (h).

Figure 3. Amount of rhodamine B extracted in batch mode using the bulk UiO MOFs (Conditions: Rhodamine B concentration, 10 mg L^{-1}. Extraction time, 15 min) (a). Extraction performance of the automated SPE of phenols using different UiO-based MOF-MMDs (Conditions: 1.5 mL of sample solution (pH= 6). Sample flow rate, 1 mL min^{-1}. Analyte concentration, 50 µg L^{-1}. Desorption solvent, 0.5 mL methanol containing 0.1 mmol L^{-1} NaOH. Desorption solvent flow rate, 1 mL min^{-1}) (b).

Figure 4. SEM micrographs of a bare PVDF disk (a) and a NP-UiO-66-NH_2-MMD (b, c). XRD patterns of a bare PVDF disk and a NP-UiO-66-NH_2-MMD (The simulated pattern of the bulk material, obtained from the crystallographic data reported by Zhao et al. [56], is shown for the sake of comparison) (d). EDS mapping of Zr of the NP-UiO-66-NH_2-MMD (e). EDS spectra of the bare PVDF disk and the NP-UiO-66-NH_2-MMD (f). Cross-section SEM micrographs of the NP-UiO-66-NH_2-MMD (g, h).

Figure 5. Desorption solvent selection for the automated SPE of phenols using the NP-UiO-66-NH_2-MMD. Conditions: sample volume, 1.5 mL (pH= 6). Sample flow rate. 1 mL min^{-1}. Analyte concentration, 50 µg L^{-1}. Desorption solvent contains 0.1 mmol L^{-1} NaOH. Desorption solvent flow rate, 1 mL min^{-1}.

Figure 6. Effect of the sample volume (a), desorption solvent volume (b), sample flow rate (c) and desorption solvent flow rate (d) on the automated SPE of phenols using the NP-UiO-66-NH_2-MMD as sorbent. Conditions: sample volume, 1.5 mL (pH= 6). Sample flow rate, 1 mL min^{-1}. Analyte concentration, 50 µg L^{-1}. Desorption solvent, 0.3 mL acetone containing 0.1 mmol L^{-1} NaOH. Desorption solvent flow rate, 1 mL min^{-1}. Unless otherwise stated in the graphs.

Figure 7. HPLC chromatograms of the direct injection of a standard spiked with the analytes and thionin (50-fold), a spiked sample (5 µg L^{-1}) with the identical analyte and thionin concentration after automated SPE using a bare PVDF disk, and a MOF-MMD containing NP-UiO-66-NH_2 crystals. Peaks: Thionin (*), 4-NP (1), 2-CP (2), 2,4-DNP (3), 2-NP (4), 2,4-DMP (5), 4-C-3-MP (6), 2,4-DCP (7).

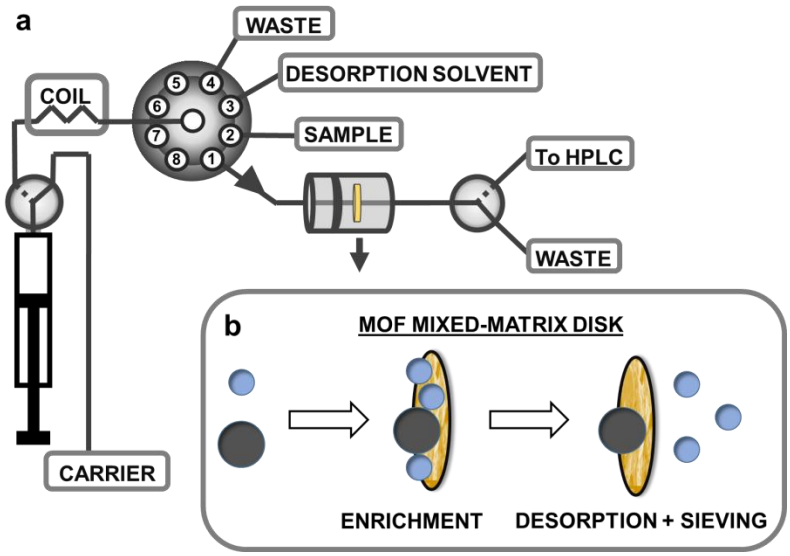

Figure 1. Representation of the developed set-up for the implementation of MOF-MMDs for automated SPE (a), and the SPE process using MOF-MMDs (b).

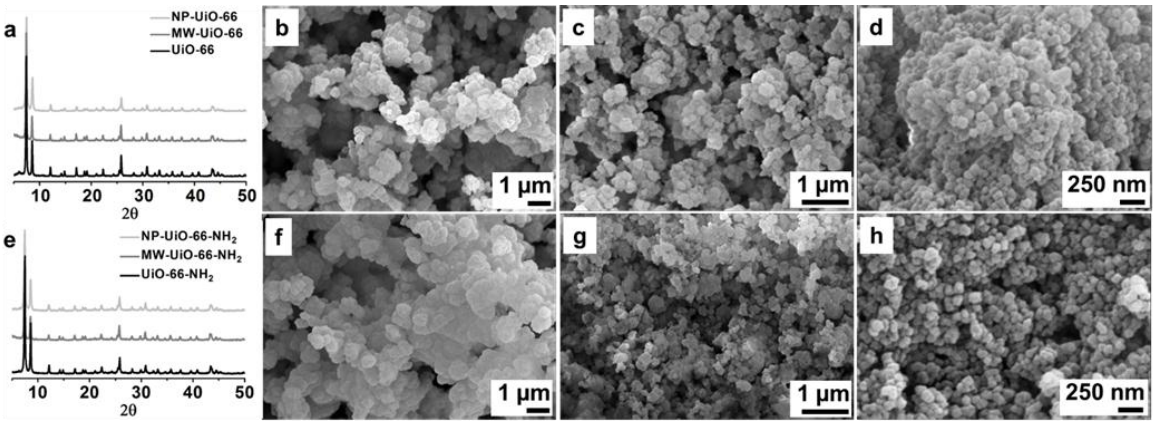

Figure 2. XRD pattern of the synthesized UiO-66 samples (a). SEM images of the prepared UiO-66 (b), MW-UiO-66 (c) and NP-UiO-66 (d). XRD pattern of the synthesized UiO-66-NH_2 samples (e). SEM images of the prepared UiO-66-NH_2 (f), MW-UiO-66-NH_2 (g) and NP-UiO-66-NH_2 (h).

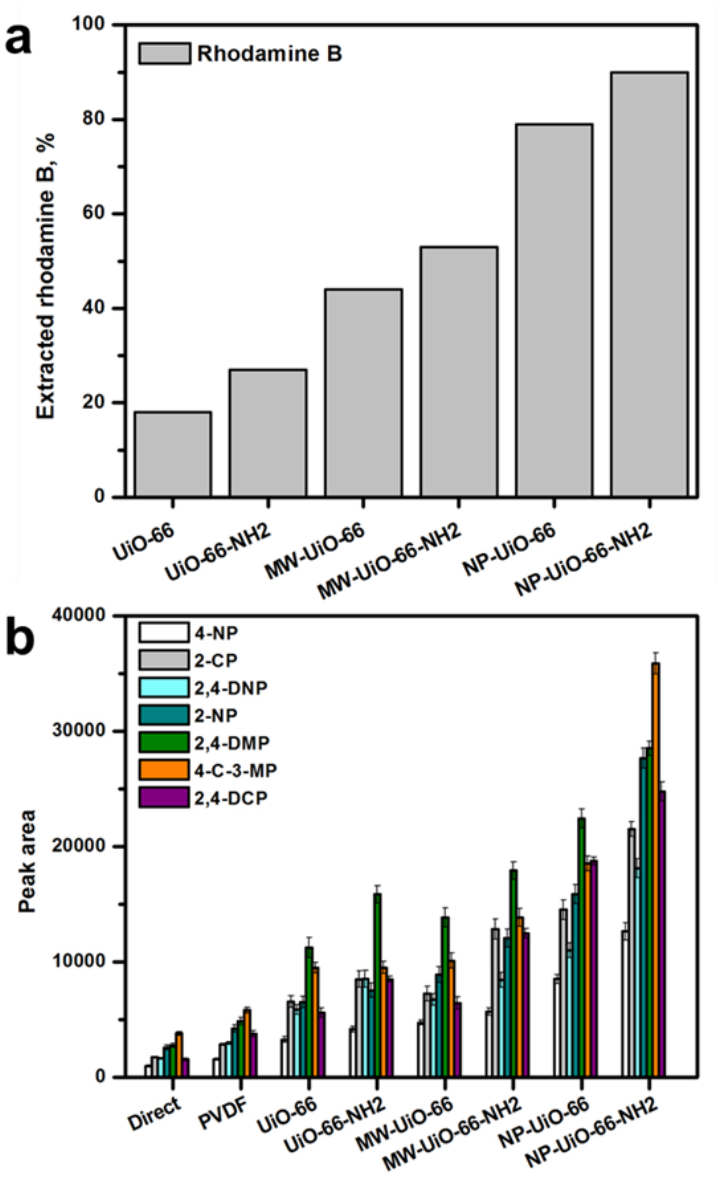

Figure 3. Amount of rhodamine B extracted in batch mode using the bulk UiO MOFs (Conditions: Rhodamine B concentration, 10 mg L^{-1}. Extraction time, 15 min) (a). Extraction performance of the automated SPE of phenols using different UiO-based MOF-MMDs (Conditions: 1.5 mL of sample solution (pH= 6). Sample flow rate, 1 mL min^{-1}. Analyte concentration, 50 µg L^{-1}. Desorption solvent, 0.5 mL methanol containing 0.1 mmol L-1 NaOH. Desorption solvent flow rate, 1 mL min-1) (b).

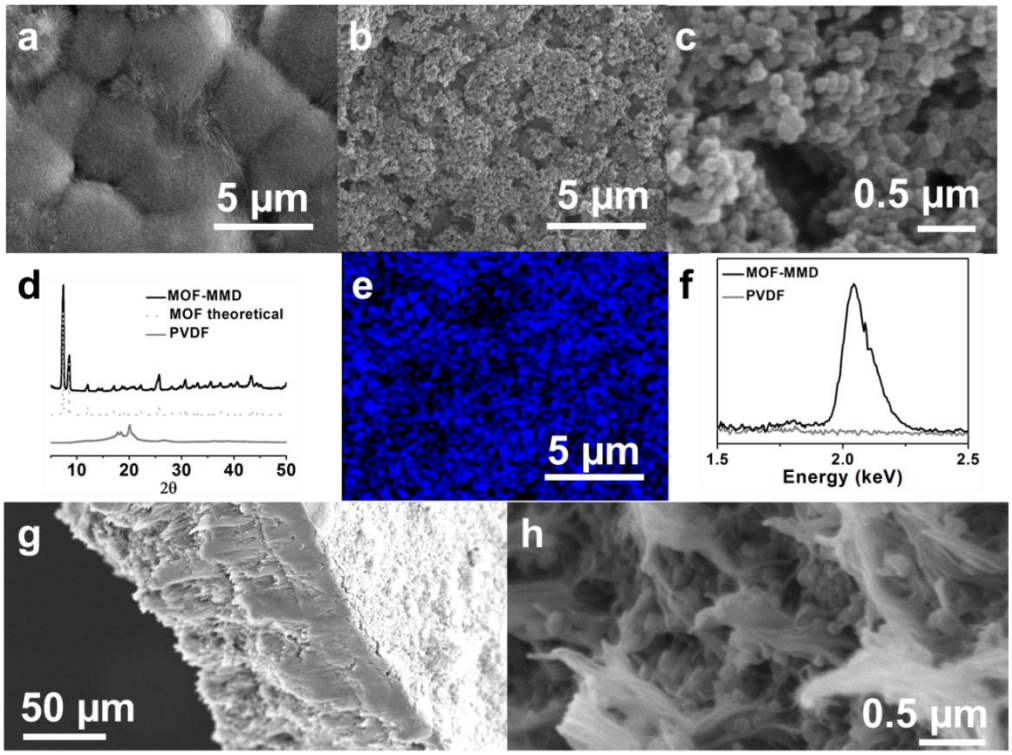

Figure 4. SEM micrographs of a bare PVDF disk (a) and a NP-UiO-66-NH_2-MMD (b, c). XRD patterns of a bare PVDF disk and a NP-UiO-66-NH_2-MMD (The simulated pattern of the bulk material, obtained from the crystallographic data reported by Zhao et al. [56], is shown for the sake of comparison) (d). EDS mapping of Zr of the NP-UiO-66-NH_2-MMD (e). EDS spectra of the bare PVDF disk and the NP-UiO-66-NH_2-MMD (f). Cross-section SEM micrographs of the NP-UiO-66-NH_2-MMD (g, h).

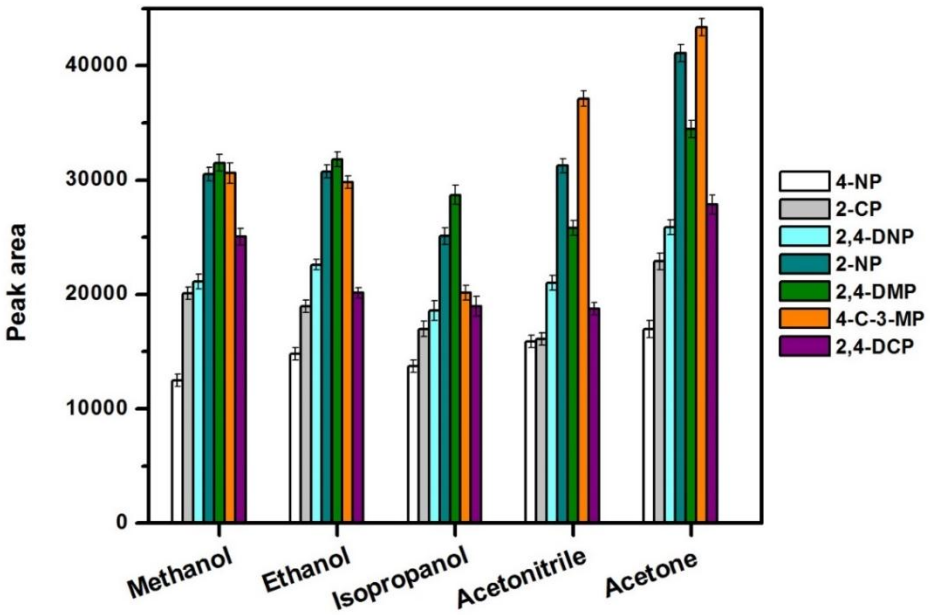

Figure 5. Desorption solvent selection for the automated SPE of phenols using the NP-UiO-66-NH_2-MMD. Conditions: sample volume, 1.5 mL (pH= 6). Sample flow rate. 1 mL min^{-1}. Analyte concentration, 50 µg L^{-1}. Desorption solvent contains 0.1 mmol L^{-1} NaOH. Desorption solvent flow rate, 1 mL min^{-1}.

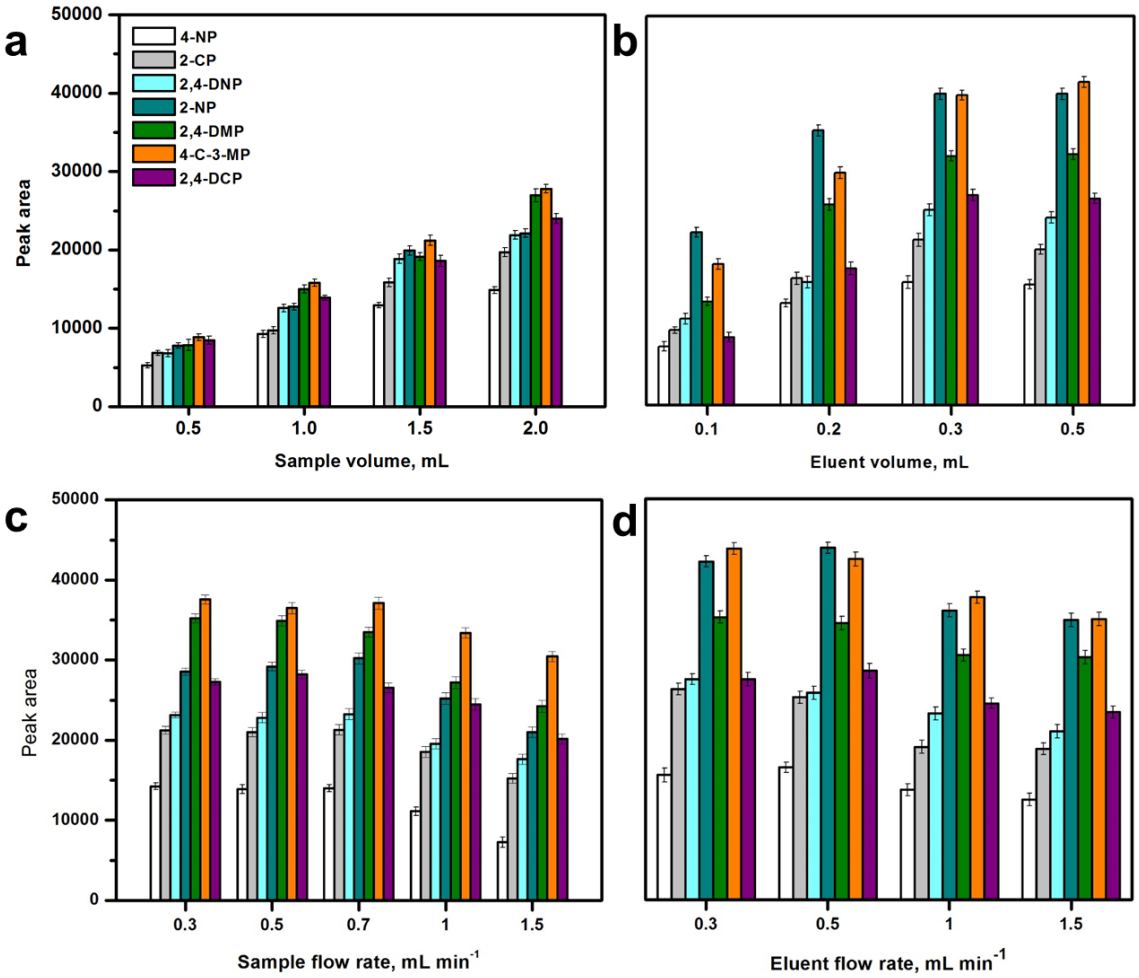

Figure 6. Effect of the sample volume (a), desorption solvent volume (b), sample flow rate (c) and desorption solvent flow rate (d) on the automated SPE of phenols using the NP-UiO-66-NH_2-MMD as sorbent. Conditions: sample volume, 1.5 mL (pH= 6). Sample flow rate, 1 mL min^{-1}. Analyte concentration, 50 µg L^{-1}. Desorption solvent, 0.3 mL acetone containing 0.1 mmol L^{-1} NaOH. Desorption solvent flow rate, 1 mL min^{-1}. Unless otherwise stated in the graphs.

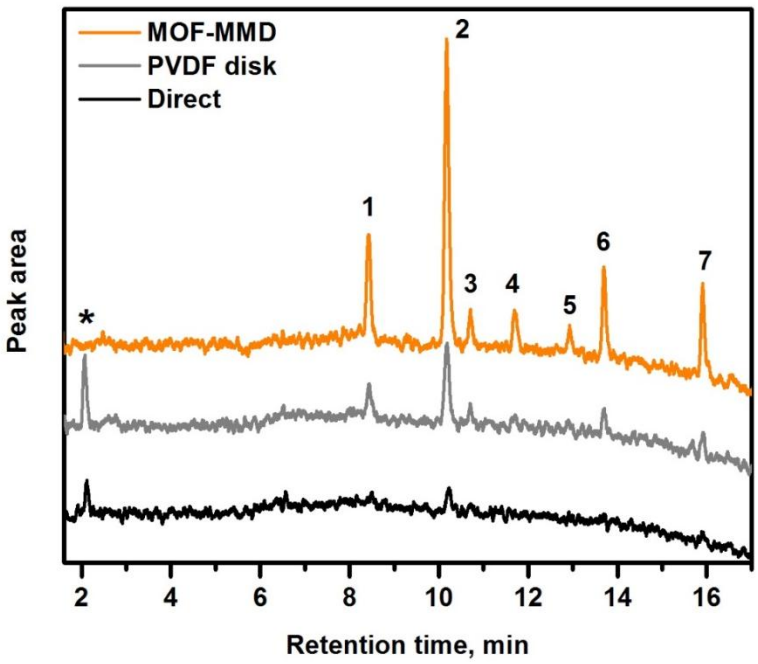

Figure 7. HPLC chromatograms of the direct injection of a standard spiked with the analytes and thionin (50-fold), a spiked sample (5 µg L^{-1}) with the identical analyte and thionin concentration after automated SPE using a bare PVDF disk, and a MOF-MMD containing NP-UiO-66-NH_2 crystals. Peaks: Thionin (*), 4-NP (1), 2-CP (2), 2,4-DNP (3), 2-NP (4), 2,4-DMP (5), 4-C-3-MP (6), 2,4-DCP (7).